Folding, Stability, and Physical Properties of the α Subunit of Bacterial Luciferase[†]

Brian W. Noland, Lawrence J. Dangott, and Thomas O. Baldwin*

Center for Macromolecular Design, the Department of Biochemistry and Biophysics, and the Chemistry Department, Texas A&M University, College Station, Texas 77843-2128, and Biochemistry Department, University of Arizona, P.O. Box 210088, Tucson, AZ 85721-0088

Received June 23, 1999; Revised Manuscript Received October 1, 1999

ABSTRACT: Bacterial luciferase is a heterodimeric (αβ) enzyme composed of homologous subunits. When the *Vibrio harveyi luxA* gene is expressed in *Escherichia coli*, the α subunit accumulates to high levels. The α subunit has a well-defined near-UV circular dichroism spectrum and a higher intrinsic fluorescence than the heterodimer, demonstrating fluorescence quenching in the enzyme which is reduced in the free subunit [Sinclair, J. F., Waddle, J. J., Waddill, W. F., and Baldwin, T. O. (1993) *Biochemistry 32*, 5036−5044]. Analytical ultracentrifugation of the α subunit has revealed a reversible monomer to dimer equilibrium with a dissociation constant of 14.9 ± 4.0 μM at 18 °C in 50 mM phosphate and 100 mM NaCl, pH 7.0. The α subunit unfolded and refolded reversibly in urea-containing buffers by a three-state mechanism. The first transition occurred over the range of 0−2 M urea with an associated free-energy change of 2.24 ± 0.25 kcal/mol at 18 °C in 50 mM phosphate buffer, pH 7.0. The second, occurring between 2.5 and 3.5 M urea, comprised a cooperative transition with a free-energy change of 6.50 ± 0.75 kcal/mol. The intermediate species, populated maximally at ca. 2 M urea, has defined near-UV circular dichroism spectral properties distinct from either the native or the denatured states. The intrinsic fluorescence of the intermediate suggested that, although the quantum yield had decreased, the tryptophanyl residues remained largely buried. The far-UV circular dichroism spectrum of the intermediate indicated that it had lost ca. 40% of its native secondary structure. N-Terminal sequencing of the products of limited proteolysis of the intermediate showed that the C-terminal region of the α subunit became protease labile over the urea concentration range at which the intermediate was maximally populated. These observations have led us to propose an unfolding model in which the first transition is the unfolding of a C-terminal subdomain and the second transition represents the unfolding of a more stable N-terminal subdomain. Comparison of the structural properties of the unfolding intermediate using spectroscopic probes and limited proteolysis of the α subunit with those of the αβ heterodimer suggested that the unfolding pathway of the α subunit is the same, whether it is in the form of the free subunit or in the heterodimer.

The classical investigations of Anfinsen and colleagues clearly documented the principle that the information that dictates the correct three-dimensional fold of a protein resides in the sequence of amino acids that comprise the polypeptide (*1*). In the intervening years, much evidence has been accumulated that supports the so-called thermodynamic hypothesis, and it seems clear today that many, if not most, small globular proteins reside at a global minimum of free energy. Wetlaufer has suggested that larger proteins, many of which have domains that fold independently, also reside at global minima of free energy, differing from smaller proteins only in that they are assemblies of the independently folding domains (*2*). However, it is also apparent today that for some, and perhaps many, large, more complex proteins, kinetic factors play a critical role in dictating the final structure (*3*). Native structures obviously must have sufficient kinetic stability to exist on a biological time scale, but it appears obvious that they need not be at a global minimum of free energy.

Bacterial luciferase is a flavin monooxygenase that catalyzes the reaction of $FMNH_2$, O_2, and an aliphatic aldehyde to yield oxidized flavin, the carboxylic acid, and blue green light (see ref *4* for a review). The enzyme is a heterodimer consisting of two homologous subunits (*5*), α and β, with molecular weights of 40 153 and 36 349, respectively (*6*, *7*). Even though the subunits are homologous (*5*) and both can independently support a very low quantum yield bioluminescence reaction (*9*, *45*, *46*), it is clear that the active center resides on the α subunit (*4*, *8*). The high quantum yield bioluminescence reaction requires formation of the heterodimer (*4*).

The subunits fold into the well-known $(\beta/\alpha)_8$ motif (see Figure 1) and pack together through an extensive interface that has at its core a novel sort of parallel 4-helix bundle (*10*). The β subunit self-associates very slowly to yield the homodimer, a structure that is resistant to unfolding in 5 M urea (*11*). The dissociation of the homodimer is extremely slow in neutral buffers and modest temperatures, with a dissociation half-time of ca. 1 million years (*11*). The structure of the homodimer has been determined to 1.95 Å

[†] Supported in part by grants from the National Science Foundation (MCB-9513429), the Office of Naval Research (N0001496-1-0087), the Robert A. Welch Foundation, and Amgen, Inc. B.W.N. was supported by NIH Chemistry/Biology Interface Training Grant GM08523.

* To whom correspondence should be addressed. Phone: (520) 621-9185. Fax: (520) 626-9204. E-mail: tbaldwin@u.arizona.edu.

10.1021/bi991449b CCC: $18.00
Published on Web 11/10/1999

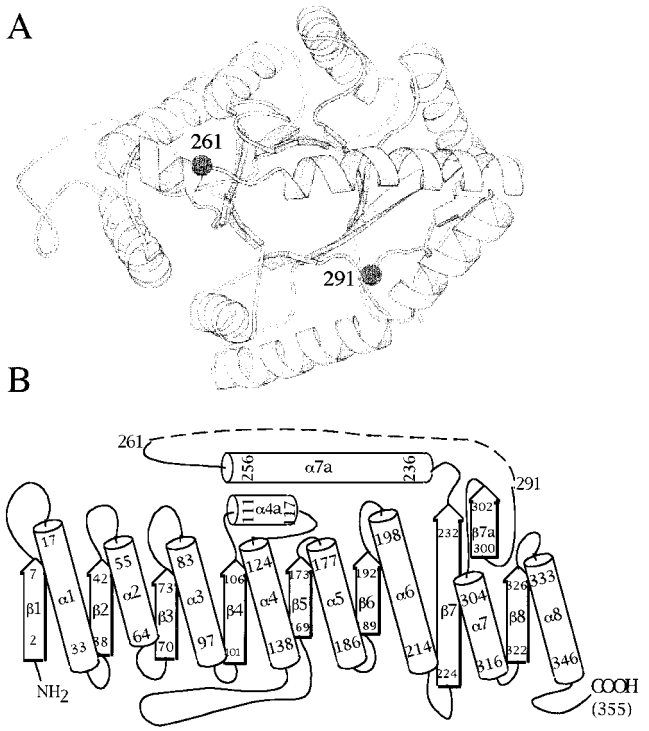

FIGURE 1: (A) Structure of the α subunit of bacterial luciferase from the 1.5 Å heterodimer crystal structure (*40*). Secondary structural elements are shown to illustrate the overall $(\beta/\alpha)_8$ architecture of the α subunit. The α carbon trace of the α subunit was generated using MOLESCRIPT (*41*). The locations of residues 261 and 291 which define the limits of the disordered loop are indicated. (B) Topographic diagram of the secondary structure of the α subunit of luciferase (from ref *42*, reproduced with permission).

resolution (*12*). The β subunits in the homodimer are very similar to each other and to the β subunit in the heterodimer, yet both subunits of the heterodimer appear to unfold virtually completely in 5 M urea, while the homodimer appears to be insensitive to 5 M urea (*10*−*12*).

It has been demonstrated by Clark et al. (*13*) that the luciferase heterodimer unfolds by a three-state mechanism with an intermediate that is maximally populated at 2.1 M urea. This intermediate is dimeric, with a reduced CD signal at 222 nm and an increased intrinsic fluorescence quantum yield relative to the protein in the absence of urea. The change in free energy associated with the first transition is about 4.52 kcal/mol and that of the second is about 19.7 kcal/mol in 50 mM phosphate, pH 7.0 at 18 °C.

The β subunit folding behavior, independent of the heterodimer, has been described by Sinclair et al. (*11*). As a result of the extraordinary kinetic stability of the β subunit homodimer, the folding and unfolding transitions are noncoincident. This hysteresis in the denaturation and renaturation data was interpreted as evidence for a high kinetic barrier between the folded and unfolded states. Thermodynamically, β_2 would prefer to be in the unfolded state in 5 M urea, but because of the high activation barrier between the folded and unfolded states, β_2 remains folded in 5 M urea.

Relatively little has been described about the folding or structure of the free α subunit. In previous spectroscopic studies of the α subunit, which contains most of the tryptophanyl residues, it was shown that the spectral properties of the free α subunit are similar to those of the $\alpha\beta$ heterodimer, suggesting that the α subunit structure is similar to that of the α subunit in the heterodimer (*9*). The α subunit in its native state is competent to associate with refolding β subunit to yield active enzyme. Therefore, the α subunit may be considered a folding intermediate in the heterodimer folding reaction. Understanding of a folding pathway requires knowledge of the structures of intermediates. The purpose of the work described here was to begin to develop an understanding of the structure of the α subunit and the differences in structure between the free subunit and the heterodimer imposed by interactions with the β subunit. In the course of these investigations, we discovered that the α subunit, like the β subunit, can form a homodimer. However, unlike the β subunit homodimer, the α subunit homodimer was only weakly associating and in rapid equilibrium with the monomer. As with the heterodimer, the α subunit unfolded at 18 °C, pH 7.0, by a three-state mechanism, with an intermediate that was well populated at 2.0 M urea. The α subunit intermediate, like the heterodimeric intermediate, had a reduced CD signal at 222 nm and an altered intrinsic fluorescence quantum yield. By limited proteolysis of both the heterodimeric intermediate and the α subunit intermediate, we found that a C-terminal subdomain of the α subunit was partially unfolded in 2 M urea, both as the free subunit and in the heterodimer; association with the β subunit afforded the C-terminal subdomain of the α subunit ca. 2 kcal/mol additional stability.

MATERIALS AND METHODS

Materials. Ultrapure urea was purchased from ICN. TLCK-treated chymotrypsin was obtained from Worthington Enzymes. Dithiothreitol (DTT) and 10% Tween 20 were purchased from Boehringer Mannheim, NaH_2PO_4 and K_2HPO_4 from J. T. Baker, and chromatographic media from Pharmacia Biotech. All other chemicals were of reagent grade or better.

Stock Solutions and Buffers. Buffers designated phosphate buffer were made at the indicated concentrations by mixing and diluting the appropriate amounts of 1 M solutions of NaH_2PO_4 and K_2HPO_4. Phosphate buffers used in purification procedures were pH 7.0 and contained 0.5 mM DTT and 1 mM EDTA. Solutions of 10 M urea were prepared as described by Pace et al. (*14*) in 50 mM phosphate, 1 mM DTT, and 0.005% Tween 20, pH 7.0. Solutions were prepared fresh daily and filtered through a 0.22 μm filter prior to use. The buffer used for the CD measurements was 25 mM phosphate, 1 mM EDTA, and 0.1 mM DTT, pH 7.0. Limited proteolysis was carried out in 50 mM phosphate and 1 mM DTT, pH 7.0. The buffer used in analytical ultracentrifugation was 50 mM phosphate, 100 mM NaCl, and 1.0 mM DTT, pH 7.0.

Expression and Protein Purification. Protein was expressed in *Escherichia coli* strain ALF1 that was prepared by transforming *E. coli* strain GYR1 with the pBN1 plasmid. Plasmid pBN1 is a derivative of the pJHD500 plasmid (*15*) from which most of the *luxB* gene, which encodes the β subunit, had been removed. The plasmid pBN1 was constructed by excising the region in pJHD500 from 2560 to 3398 using standard recombinant DNA methods. Protein expression from ALF1 was performed as described by Thomas and van Tilburg (*16*). The crude lysate was brought

to 40% saturation with $(NH_4)_2SO_4$, then centrifuged at 10 000 rpm for 45 min. The resulting supernatant was adjusted to 75% saturation with $(NH_4)_2SO_4$, then centrifuged at 10 000 rpm for 45 min. This pellet was suspended in 200 mM phosphate buffer and dialyzed against three changes of a 20-fold excess of the same buffer. Dialyzed protein was applied to a DEAE-Sepharose column equilibrated in 200 mM phosphate buffer. Protein was eluted by a linear gradient of three column volumes from 200 to 700 mM phosphate. Fractions were pooled based on visualization of protein by Coomassie blue staining of protein in polyacrylamide gels (*17*). The pool was dialyzed against a 20-fold excess of 100 mM phosphate buffer through three changes and then applied to a Q-Sepharose column equilibrated in 100 mM phosphate buffer. Protein was eluted by a linear gradient consisting of 10 column volumes from 100 to 400 mM phosphate. Fractions were pooled based on analysis by polyacrylamide gel electrophoresis. Purified protein was dialyzed against a 20-fold excess of 50 mM phosphate buffer for three changes. The dialyzed protein was concentrated to ca. 20 mg/mL using a stirred cell under 30 psi N_2 pressure and a YM10 membrane (Amicon). Concentrated protein was flash-frozen under liquid N_2 and stored at −20 °C.

Equilibrium Denaturation Experiments. Equilibrium denaturation experiments were performed as described by Pace et al. (*14*). Protein stocks were prepared at 10 times the final concentration in 50 mM phosphate buffer as described above (*13*). The final protein solutions in urea were prepared by mixing appropriate volumes of the protein stock, 10 M urea stock in 50 mM phosphate buffer, and 50 mM phosphate buffer.

Fluorescence emission was monitored using an SLM-Aminco 8000C spectrofluorimeter with a 1 cm quartz cuvette. Emission spectra were analyzed over the wavelength range 300−400 nm with an excitation wavelength of 280 nm. Data reported represent the average of two spectra. Spectra were corrected for background signal contribution. Samples were maintained at 18 °C during all measurements.

Circular dichroism measurements at 222 nm for the equilibrium denaturation experiments were obtained using an Aviv 62DS spectropolarimeter, with samples maintained at 18 °C. Quartz cuvettes of either 1 cm path length (for the 10 μg/mL sample) or 0.5 cm path length (all other samples) were used for monitoring the equilibrium unfolding transitions. Circular dichroism spectra in the far UV (180−250 nm) were recorded using a 1 mm quartz cuvette, and those in the near-UV (250−330 nm) were recorded using a 1 cm cuvette. Each of the spectra presented was the average of five scans.

Limited Proteolysis. Samples of α subunit and of luciferase (1 mg/mL in limited proteolysis buffer) were exposed to chymotrypsin (10 μg/mL) for 15 min and the reaction quenched by the addition of 100 μL of the digest mix to an equivalent volume of boiling SDS−PAGE sample buffer (*17*). Aliquots of samples were applied to a polyacrylamide gel (8 × 10 × 0.05 cm) in SDS-containing buffers, and fragments were resolved electrophoretically at a constant voltage of 150 V. The protein bands in the gels were stained with Coomassie brilliant blue or transferred electrophoretically onto PVDF membranes for N-terminal sequencing (*18*).

N-Terminal Peptide Sequencing. The proteins were separated by electrophoresis in polyacrylamide gels in the presence of SDS (*19*) transferred electrophoretically to PVDF membranes by the method of Matsudeira (*19*). The protein bands were visualized using Coomassie blue R-250, excised from the membrane, and subjected to automated Edman sequencing on a Hewlett-Packard G1005A Protein Sequencer with an in-line Hewlett-Packard 1090 LC for amino acid analysis. All blotting and microsequencing procedures were performed by the Protein Chemistry Laboratory at Texas A&M University.

Analytical Ultracentrifugation. Sedimentation equilibrium experiments were carried out using a Beckman XL-A analytical ultracentrifuge. Samples were dialyzed overnight at 4 °C against 50 mM phosphate buffer containing 100 mM NaCl and 0.5 mM DTT. Protein samples and dialysate as blanks were allowed to come to equilibrium at 15 000, 18 000, or 25 000 rpm at 18 °C. Scans of the absorbance at 280 and 252 nm as a function of radial position were taken and equilibrium was assumed to be reached when consecutive scans 4 h apart superimposed.

Sedimentation Equilibrium Data Analysis. Sedimentation equilibrium data were fit to both a model for a single sedimenting species, eq 1, and a monomer−dimer associating system model, eq 2,

$$A_r = A_0 \exp\{[M(1 - \nu\rho)\omega^2/2RT][r_0 - r]\} + E \quad (1)$$

$$A_r = A_0 \exp\{[M(1 - \nu\rho)\omega^2/2RT][r_0 - r]\} + (A_0)^2 K_a \exp\{[M(1 - \nu\rho)\omega^2/2RT][r_0 - r]\} + E \quad (2)$$

where A_r is the absorbance at any radial position, r is the radial position, A_0 is the absorbance at the reference radial position, r_0 is the reference radial position, K_a is association constant, ν is partial specific volume of the sedimenting species, ρ is solvent density, ω is angular velocity, R is the ideal gas constant, and T is the absolute temperature. The partial specific volume, ν, for the α subunit, 0.731 mL/g, was calculated based on the amino acid composition (*6*) as described by Cohn and Edsall (*20*). The value of ρ, 1.007 42 g/mL, was determined from standard tables (*21*).

Average Emission Wavelength. Average emission wavelength $\langle\lambda\rangle$ was calculated from fluorescence emission spectra obtained in the emission range 300−400 nm with an excitation wavelength of 280 nm using eq 3 (*22*):

$$\langle\lambda\rangle = (\sum F_i\lambda_i)/\Sigma F_i \quad (3)$$

where F_i is the fluorescence intensity at wavelength λ_i. Average emission wavelength, unlike measurements done at a single wavelength, reflects not only changes in intensity but also changes in the spectral envelope. Because average emission wavelength is an integral measurement, it is less susceptible to noise than single wavelength measurements (*22*).

Analysis of Equilibrium Denaturation Data. Equilibrium denaturation data were best described by including an intermediate in the unfolding model:

$$N \overset{K_1}{\rightleftharpoons} I \overset{K_2}{\rightleftharpoons} U \quad (4)$$

N denotes the protein in its native state, I is the intermediate, and U is the unfolded state. We can define the mole fraction of each state by dividing the concentration of each species

by the total protein concentration P_T:

$$P_T = [N] + [I] + [U] \quad (5)$$

$$f_N = [N]/P_T \quad (6)$$

$$f_I = [I]/P_T \quad (7)$$

$$f_U = [U]/P_T \quad (8)$$

The sum of the mole fractions of all species must equal 1.

$$f_N + f_I + f_U = 1$$

The equilibrium constant for each step can be defined in terms of mole fractions as

$$K_1 = f_I/f_N \quad (9)$$

$$K_2 = f_U/f_I \quad (10)$$

and likewise, mole fractions can be expressed in terms of the equilibrium constants:

$$f_N = 1/(1 + K_1 + K_1K_2) \quad (11)$$

$$f_I = K_1/(1 + K_1 + K_1K_2) \quad (12)$$

$$f_U = K_1K_2/(1 + K_1 + K_1K_2) \quad (13)$$

The change in Gibbs free energy, ΔG, can be assumed to be a linear function of urea concentration so that the change in free energy at any urea concentration can be obtained using

$$\Delta G_1 = \Delta G_{H_2O,1} + m_1[\text{urea}] \quad (14)$$

$$\Delta G_2 = \Delta G_{H_2O,2} + m_2[\text{urea}] \quad (15)$$

where $\Delta G_{H_2O,1}$ and $\Delta G_{H_2O,2}$ are defined as the free energy changes in the absence of denaturant and m_1 and m_2 are the slopes of the line used to extrapolate these free energies. The contributions of all states to the total amplitude are assumed to be additive, such that the total observed signal, Y_{obs}, is

$$Y_{obs} = Y_N f_N + Y_I f_I + Y_U f_U \quad (16)$$

where Y_N, Y_I, and Y_U represent the amplitude associated with each species. It was assumed that the amplitudes attributed to the native and unfolded states varied linearly with denaturant or

$$Y_N = Y'_N + m_{pre}[\text{urea}] \quad (17)$$

and

$$Y_U = Y'_U + m_{post}[\text{urea}] \quad (18)$$

where Y'_N and Y'_U are the amplitudes of the signals of the native and unfolded states in the absence of urea. The slopes of the pre- and posttransition baselines, m_{pre} and m_{post}, are proportional to the dependence of the magnitude of the spectroscopic signal of the native and denatured states, respectively, on denaturant concentration.

Data Fitting Procedures. Sedimentation equilibrium data were analyzed using eqs 1 and 2 with the nonlinear least-squares fitting engine in the program Kaleidagraph (Synergy Software, Reading, PA). Equilibrium denaturation data were analyzed using the program IGOR PRO (WaveMetrics, Lake Oswego, OR) using eqs 4−18.

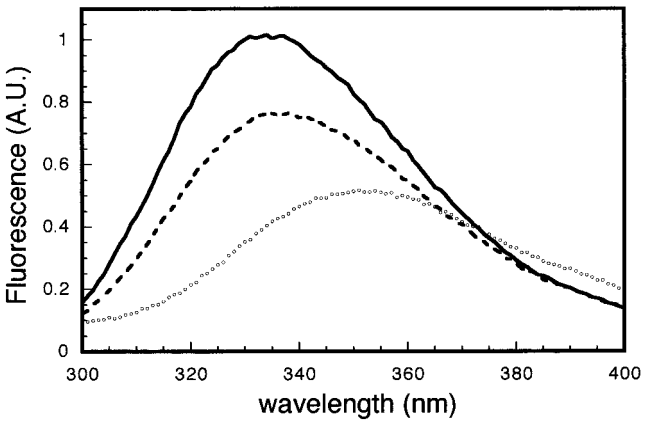

FIGURE 2: Effect of urea on the fluorescence emission spectrum. Each sample was prepared in 50 mM phosphate buffer, 1.0 mM DTT, 0.005% Tween 20, and the indicated concentration of urea. The concentration of α subunit was 25 μg/mL. Fluorescence emission data were collected from 300 to 400 nm with an excitation wavelength of 280 nm. The solid line is the protein under native conditions equilibrated in 50 mM phosphate buffer in the absence of urea. Protein equilibrated in 2 M urea is shown in the dashed trace. Protein unfolded in 6 M urea is shown in the dotted trace. Each spectrum represents the average of two 1 min scans. All spectra were corrected for background signal contribution.

RESULTS

Effect of Urea on the Fluorescence Emission Spectrum. The existence of an intermediate in the urea-induced unfolding of the α subunit of bacterial luciferase was apparent from the fluorescence emission spectra recorded in various concentrations of urea (Figure 2). Under nondenaturing conditions, the spectral maximum was at 335 nm when excited at 280 nm. In the presence of 6 M urea, the fluorescence intensity was reduced by ca. 50% and the emission maximum was red-shifted to about 355 nm, suggesting that the tryptophanyl residues were exposed to solvent water. However, in 2 M urea, the fluorescence intensity was reduced by ca. 30%, but the emission maximum had red-shifted only 2 nm, suggesting that the tryptophanyl residues in this intermediate were buried within the protein.

Effect of Urea on the Circular Dichroism Spectrum. Under nondenaturing conditions, the α subunit had a CD spectrum (Figure 3) consistent with a folded nativelike structure, as described by Sinclair et al. (*9*). In 6 M urea, the CD spectrum suggested that the protein was unfolded. However, in 2 M urea, the near-UV CD spectrum showed substantial rearrangement of the aromatic side chains, but the far-UV CD spectrum suggested only partial loss of secondary structure.

Analytical Ultracentrifugation. The solution molecular weight of the α subunit was determined by analytical ultracentrifugation (Figure 4). When the sedimentation equilibrium data were fit to the equation for a single sedimenting species (eq 1, Figure 4A) an apparent molecular weight of about 60 400 was obtained, whereas the sum of the molecular weights of the constituent amino acid residues is 40 153 (*6*). Furthermore, the residuals from this analysis (Figure 4A, top) were nonrandom. The same data fit to a monomer−dimer equilibrium (eq 2) with molecular weights

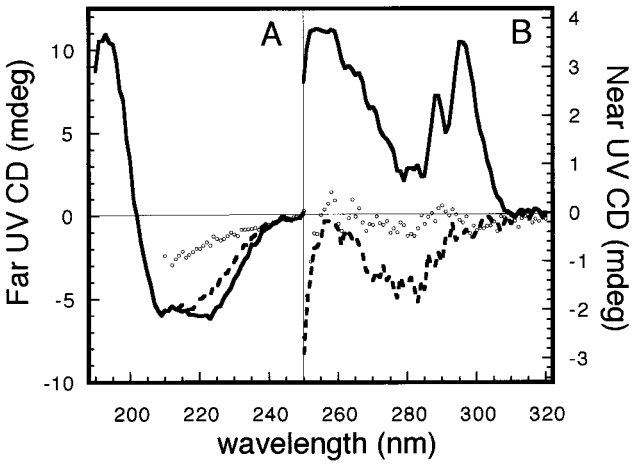

FIGURE 3: Effect of urea on the circular dichroism spectrum. Samples were equilibrated in 50 mM phosphate buffer, 1.0 mM DTT, 0.005% Tween 20, and the indicated concentration of urea. The concentration of protein for the far-UV spectrum (190−250 nm) was 8.2 μg/mL (A). The concentration of protein used for the near-UV spectrum (250−320 nm) was 0.82 mg/mL (B). Native protein, equilibrated in 50 mM phosphate buffer, is shown in the solid traces. Protein in buffer containing 2 M urea, where the intermediate is highly populated, is shown in the dashed lines. Spectra of unfolded protein in 6 M urea are shown in the dotted lines. Each spectrum represents the average of five scans.

of 40 153 and 80 306 for the two species yielded random residuals (Figure 4B, top). The dissociation constants for sedimentation equilibrium analyses at various protein concentrations and rotor speeds are shown in Table 2. The K_d determined from these data was 14.9 ± 4.0 μM.

Determination of the Conformational Stability of the α *Subunit.* Titration of the α subunit with urea (Figure 5) demonstrated an intermediate that was well-populated in the range 1.2−2.8 M urea, consistent with the spectra shown in Figures 2 and 3. When samples equilibrated in the urea-containing buffers at 18 °C for 18−24 h were analyzed by fluorescence or circular dichroism, a non-two-state unfolding transition was observed. The solid lines in Figure 5 represent the best fit to the data of a model that includes an equilibrium intermediate. The change in Gibbs free energy in buffer at 18 °C for the native to intermediate transition was 2.24 ± 0.25 kcal/mol, and for the intermediate to unfolded transition, it was 6.50 ± 0.75 kcal/mol. The *m* values for the first and second transitions were 2.44 ± 0.22 and 2.27 ± 0.16 kcal/mol/M, respectively. The pretransition baseline for the first transition (see Figure 5) was not sufficiently long to define the slope (m_{pre} in eq 17) with confidence, suggesting the possibility that, under native conditions, the protein was partially unfolded. To better define the confidence in the value for $\Delta G_{H_2O,1}$ (eq 14), the value of the slope of the pretransition baseline was varied above and below the best fit value and fixed, with the other parameters allowed to float, and the effect on the value of $\Delta G_{H_2O,1}$ determined. It was found that the value of $\Delta G_{H_2O,1}$ was not strongly dependent on the value of the pretransition baseline; m_{pre} could be varied by ±20% while the value of $\Delta G_{H_2O,1}$ did not exceed the standard deviation of the best fit values shown in Table 2. Therefore, while the determination of the thermodynamic parameters by this method was complicated by the minimal stability of the native form, the best fit values appear to be well defined by the data.

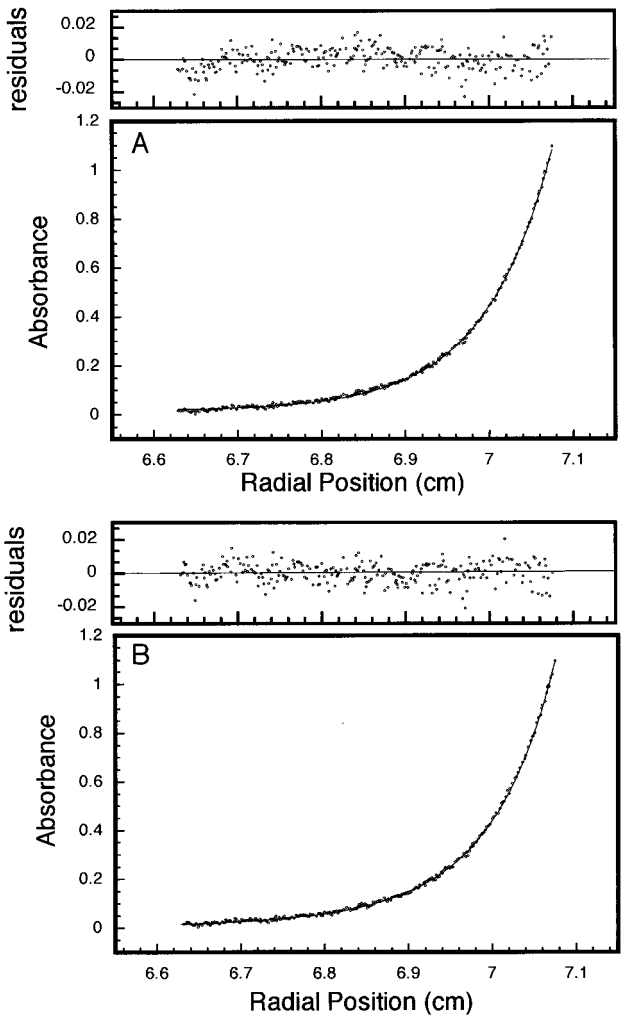

FIGURE 4: Analytical ultracentrifugation. Protein at 1.77 mg/mL was dialyzed against 50 mM phosphate buffer, 100 mM NaCl, and 1.0 mM DTT, pH 7.0, and then centrifuged at 15 000 rpm until equilibrium was achieved, approximately 20 h. Absorbance scans were taken at a radial step size of 0.001 cm, blanking at each step against dialysate. The data shown represent the average of 5 such scans. Panel A shows the data fit to a model assuming a single sedimenting species, eq 1. This fit results in a molecular weight of 60 400. The residuals for this fit are shown above panel A. Panel B shows the same data set fit to a model assuming a monomer to dimer equilibrium, eq 2. The fit yields a dissociation constant of 20.7 μM; data from similar experiments at different protein concentrations and rotor speeds yielded K_d values shown in Table 1. The residuals associated with this fit are shown above panel B.

Table 1: Dissociation Constants Obtained from Fits to the Sedimentation Equilibrium Analysis of the α Subunit of Bacterial Luciferase

speed (rpm)	protein concentration (μg/mL)	λ (nm)	K_d (μM)
15 000	1.06	280	12.7
15 000	1.42	280	16.9
15 000	1.77	280	20.7
15 000	2.00	252	16.4
18 000	0.99	252	9.13
18 000	2.00	252	16.0
18 000	0.496	252	9.77
25 000	0.496	252	17.8
avg ± std deviation			14.9 ± 4.0

The effect of protein concentration for these processes was investigated. Panels A−E of Figure 5 present the unfolding titrations with the α subunit at 10 to 30 μg/mL in 5 μg/mL

Table 2: Thermodynamic Parameters Obtained from Equilibrium Denaturation of the α Subunit of Bacterial Luciferase

protein concentration (μg/mL)	spectroscopic probe[a]	$\Delta G_{H20,1}$ (kcal/mol)	m_1 (kcal/mol/M)	$\Delta G_{H20,2}$ (kcal/mol)	m_2 (kcal/mol/M)
10	CD	2.36	2.26	6.04	2.18
10	AEW	2.25	2.47	7.19	2.47
15	CD	2.59	2.74	5.66	2.06
15	AEW	2.44	2.39	6.66	2.33
20	CD	2.05	2.03	5.60	2.22
20	AEW	2.33	2.69	6.34	2.25
25	CD	2.30	2.46	5.84	2.06
25	AEW	2.09	2.63	7.17	2.38
30	CD	1.68	2.25	6.59	2.20
30	AEW	2.27	2.44	7.90	2.55
mean ± std dev		2.24 ± 0.25	2.44 ± 0.22	6.50 ± 0.75	2.27 ± 0.16

[a] CD = circular dichroism at 222 nm, AEW = average emission wavelength calculated from eq 3 using fluorescence emission from 300 to 400 nm with excitation at 280 nm.

increments. Over this concentration range (0.25−0.75 μM) and under nondenaturing conditions, the expected amount of dimer ranged between ca. 1.7 and 5.1%. Titration of the protein with urea would be expected to shift the monomer−dimer equilibrium toward the monomer, thereby further decreasing the small fraction of dimer present under nondenaturing conditions. As can be seen from the data in Figure 5 and Table 2, there is experimental variation in the measured unfolding transitions, but there is no systematic variation with concentration, as expected based on the small fraction of dimer under initial conditions. As shown in Table 2, the best fit parameters show no consistent variation with protein concentration.

Limited Proteolysis. We have employed limited proteolysis to probe the structure of the intermediate formed in 2 M urea and to compare that structure with the native structure of the α subunit. Primarily on the basis of spectroscopic data, Sinclair et al. (*9*) concluded that the structure of the free α subunit is very similar to that of the α subunit in the αβ heterodimer. When the heterodimer is exposed to any of a wide variety of proteases, the enzyme is rapidly inactivated due to cleavage at one or more sites within the disordered loop of the α subunit (residues 262−290; refs *23* and *24*), with subsequent hydrolysis of bonds in the residues 115−125 region of the α subunit (*24*, *6*). A comparison of the limited proteolysis patterns of the free α subunit and the α subunit of the heterodimer using chymotrypsin is shown in Figure 6 A and panel B, lanes 1 and 2. The similarity in the patterns of fragmentation suggested that the structure of the α subunit was the same or very similar between the free subunit and that in the complex with the β subunit.

The changes in structure of the α subunit resulting from equilibration in 1 and 2 M urea were investigated using chymotrypsin as a probe (Figure 6B). In the presence of urea, a large proteolytic fragment was generated that was not generated when the α subunit was exposed to chymotrypsin in buffer with no urea. The size of the fragment suggested that, in the presence of urea, one of the termini was exposed and sensitive to attack by the protease. Amino acid sequence analysis of the large fragment yielded the sequence Met-Lys-Phe-Gly-Asn-, the sequence of the amino terminus of the α subunit, demonstrating that the new protease-sensitive region was near the C-terminus of the protein.

DISCUSSION

The α and β subunits of bacterial luciferase are homologous (*5*), and, as expected based on the homology, these two proteins have the same three-dimensional fold (*10*). In the biologically active structure, the αβ heterodimer, the subunit interface is extremely highly conserved, giving rise to a pseudo-2-fold rotation axis of symmetry at the interface. It was therefore not surprising to find that the β subunit self-associates, forming a very stable β_2 homodimer (*11*). The structure of the β_2 homodimer has been solved to high resolution (*12*, *25*) demonstrating that the positions of the amino acid side chains of the β subunit are essentially identical in both complexes. That is, the structure of the β subunit of bacterial luciferase is the same whether it is self-associated in the homodimer or associated with the α subunit in the heterodimer.

In the folding and assembly of the bacterial luciferase heterodimer, the α subunit has been shown to behave as a stable monomer. Native α subunit can interact with refolding β subunit to yield the heterodimer (*26*). However, the native β subunit, which is homodimeric, does not associate with refolding α subunit due to the exquisitely slow dissociation of the homodimer under nondenaturing conditions (*11*). The ability of the α subunit to form a homodimer was first demonstrated by Sinclair (*27*). We have repeated and expanded those experiments and report the results here. Indeed, the α subunit homodimer is weakly associated and appears to be in rapid equilibrium with the monomeric subunit. It remains to be determined whether the structure of the α subunit is altered significantly by association with β or by formation of the homodimer. However, the results of our experiments, reported here, suggest that the structure the free α subunit is essentially the same as that of the α subunit component of the heterodimer.

Equilibrium unfolding studies of the αβ heterodimer have shown both the existence of a well-populated intermediate and a strong protein concentration dependence of the second transition (*13*). The intermediate observed in unfolding of the heterodimer has a reduced far-UV circular dichroism signal and an increased intrinsic fluorescence. The intermediate is heterodimeric; the equilibrium between the native enzyme and the intermediate is not protein concentration dependent. The second step in the unfolding of the heterodimer is strongly concentration dependent, indicative of subunit association/dissociation. The urea-induced unfolding of the α subunit was also three-state, and the well-populated intermediate was formed over approximately the same urea concentration range as the intermediate observed in the unfolding of the heterodimer (Figure 7). However, unlike

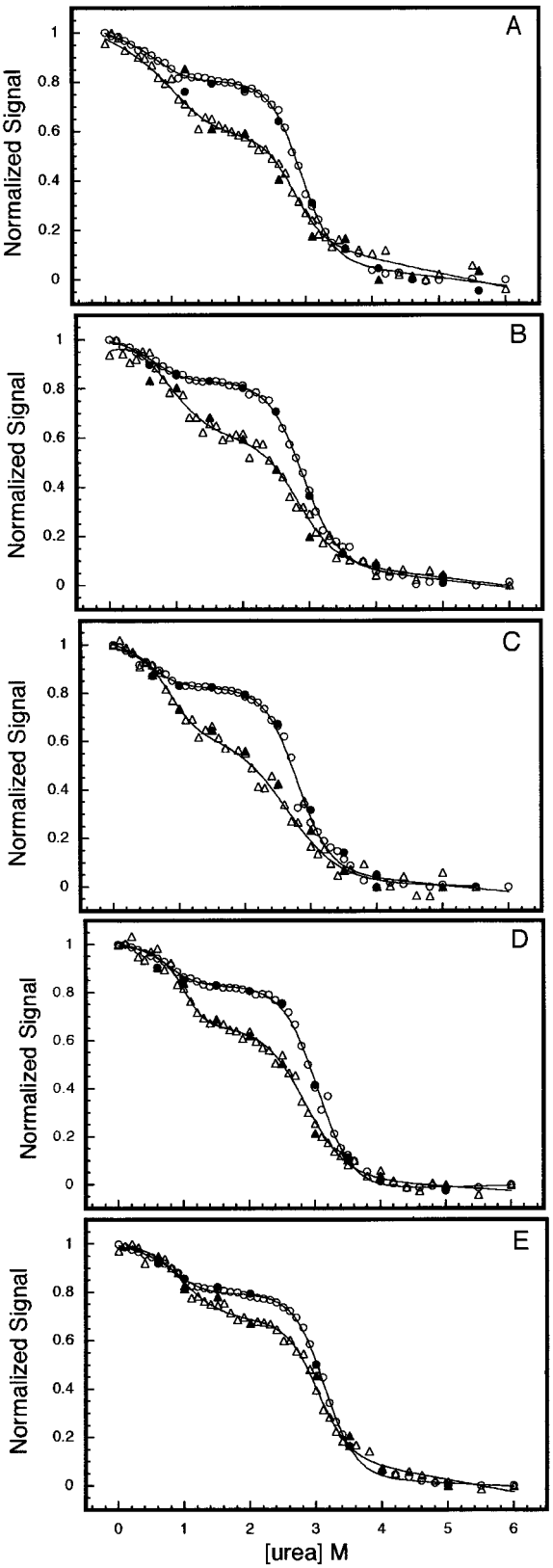

FIGURE 5: Determination of the conformational stability of the α subunit. Fluorescence average emission wavelength was calculated using eq 3 over an emission range of 300−400 nm with an excitation wavelength of 280 nm, circles. Circular dichroism was monitored at 222 nm, triangles. The protein concentrations in panels A−E were 10, 15, 20, 25, and 30 μg/mL, respectively. Filled symbols represent refolding of protein denatured in 6 M urea to the indicated concentration of urea to show reversibility. Solid lines represent nonlinear least squares best fits of the data to eq 16 as described in the Materials and Methods.

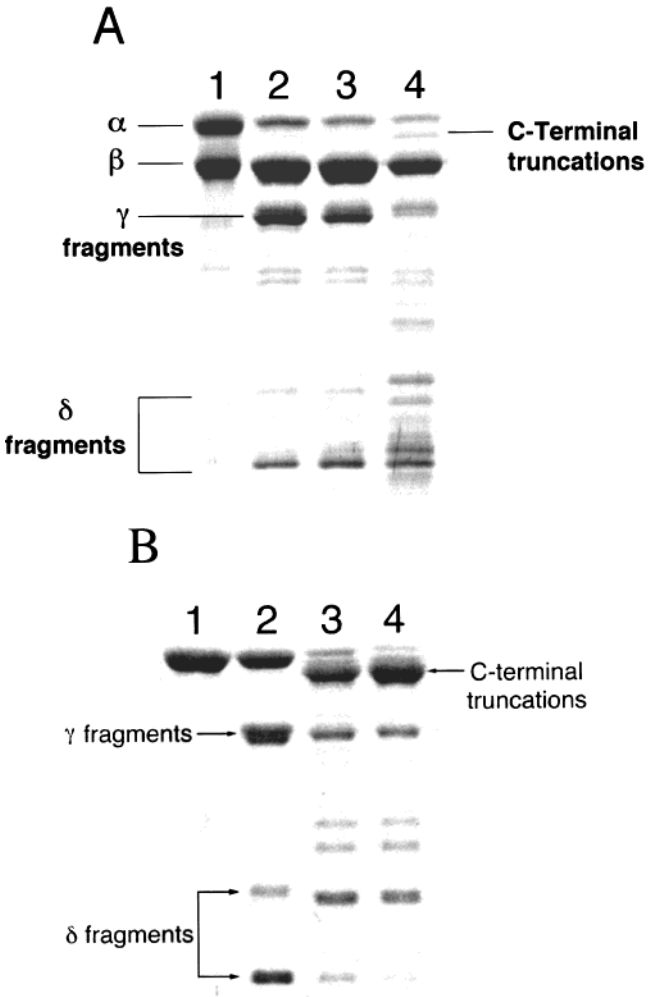

FIGURE 6: Limited proteolysis. Samples (200 μL) of 1 mg/mL α subunit and separate samples of $\alpha\beta$ luciferase, prepared in 50 mM phosphate buffer, 1.0 mM DTT, pH 7.0, and the indicated concentration of urea, were incubated for 20 h at 18 °C. Proteolysis was initiated by the addition of 10 μL of 1 mg/mL chymotrypsin. The proteolysis reaction was quenched after 15 min by adding 100 μL of the reaction mix to 100 μL of boiling SDS−PAGE buffer. Samples were boiled for an additional 5 min following the quench. An aliquot of each sample was applied to a 12% polyacrylamide gel with a 4.8% stacking gel. Electrophoresis was carried out at a constant voltage of 150 V for 1.5 h. The SDS−PAGE gel was then stained with Coomassie brilliant blue. (A) Lane 1, undigested luciferase; lane 2, native luciferase treated with chymotrypsin; lanes 3 and 4, luciferase in 1 and 2 M urea, respectively, treated with chymotrypsin. (B) Lane 1, undigested α subunit; lane 2, native α subunit treated with chymotrypsin; lanes 3 and 4, α subunit in 1 and 2 M urea, respectively, treated with chymotrypsin. The locations of the γ [residues 1−280/282 (*23*, *24*, *6*)] and δ [C-terminal (*23*, *24*, *6*)] fragment families are indicated. The location of fragments resulting from the C-terminal truncations, as determined by Edman sequencing, are indicated.

the heterodimer, the second transition did not show the same strong concentration dependence over the protein concentration range used here. Under the conditions of these experiments, the α subunit was largely monomeric.

Understanding of the folding of a protein requires knowledge of the structures of intermediates that form on the folding pathway. In the folding of both the luciferase heterodimer and the luciferase α subunit, an intermediate is well-populated in ca. 2 M urea at 18 °C, pH 7.0. For both the α subunit intermediate and the heterodimeric intermediate, the environment of the tryptophanyl residues changed

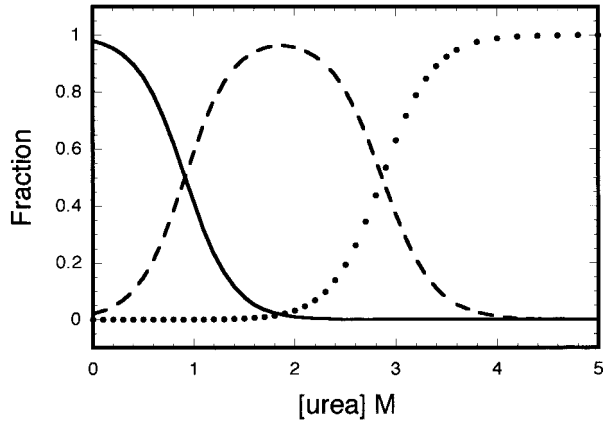

FIGURE 7: Theoretical population distribution of α subunit species as a function of urea. The fraction of each species as a function of urea was calculated using eqs 11−13 and the mean best fit parameters shown in Table 2. Fraction native, solid line; fraction intermediate, dashed line; fraction unfolded, dotted line.

without becoming exposed to solvent in response to the shift from buffer to 2 M urea. In addition, the far-UV circular dichroism signal was reduced consistent with the partial loss of secondary structure. To obtain a higher resolution understanding of the structural rearrangements that occur in the native to intermediate transition, we used limited proteolysis, a method that has been extensively used to probe activity-related conformational changes in the enzyme (*4*). Exposure of the native enzyme to chymotrypsin causes rapid inactivation of the enzyme and hydrolysis of a limited series of bonds within the protease labile loop of the α subunit (*28*−*31*) and slower hydrolysis at a second site. The Phe280−Val281 and Leu282−Lys283 bonds seem to be cleaved at comparable rates, leading to loss of activity. Subsequent hydrolysis of the Phe117−Gly118 bond completes the limited proteolysis of the luciferase heterodimer (*23*, *24*). Limited proteolysis of the α subunit under similar conditions resulted in cleavage of the same set of peptide bonds as in the α subunit in the heterodimer, the only major difference being the increased rate of hydrolysis of the Phe117−Gly118 bond in the free subunit. When the α subunit equilibrated in 2 M urea (Figure 6) was exposed to chymotrypsin, a new set of peptide bonds near the C-terminus was exposed, in addition to those that were exposed under nondenaturing conditions. The α subunit in the heterodimer equilibrated in 2 M urea showed the same alteration in protease sensitivity (Figure 6A). The *β* subunit appears to be insensitive to limited proteolysis under these conditions. These observations suggest that the structural rearrangements are the same or very similar in both the free α subunit and the α subunit in the heterodimer following a shift from buffer to 2 M urea.

The structural role of the *β* subunit in the α*β* heterodimer appears to be to stabilize and to reduce the conformational fluctuations of the α subunit. The first transition in unfolding of the heterodimer has a Gibbs free-energy change of about 4.5 kcal/mol for the heterodimer and 2.24 kcal/mol for the α subunit. The ability of the *β* subunit to stabilize the C-terminal domain of the α subunit must be due to through-protein interactions, since the C-terminal domain of the α subunit is on the side opposite the subunit interface. The *β* subunit also appears to reduce the conformational flexibility of the α subunit. The α subunit has the same protease labile bonds, both as the free subunit and bound to *β*. However, the rate of hydrolysis of these exposed bonds is greater for the free subunit, suggesting a higher degree of conformational flexibility. Clark (*32*) has used fluorescence quenching analysis to probe the conformational differences between the free α subunit and the heterodimer. The intrinsic fluorescence of the heterodimer is predominantly from the α subunit (*9*). With both iodide and acrylamide as quenchers, Clark found that the tryptophan residues of the free α subunit were more accessible than the tryptophan residues in the heterodimer. However, in the presence of 2 M urea, the accessibility of the tryptophan residues to the quenchers was essentially the same for both the heterodimer and the α subunit (*32*).

Folding intermediates have been observed in other TIM barrel proteins. The TIM barrel proteins in the tryptophan biosynthetic pathway, phosphoribosyl anthranilate isomerase [PRAI (*33*, *34*)], the α subunit of tryptophan synthase [α-TS (*35*, *36*)], and indolglycerol phosphate synthase [IGPS (*37*)] all have equilibrium folding intermediates. Organophosphate hydrolase is a highly stable dimeric TIM barrel which has been shown to have a homodimeric folding intermediate similar to that reported for the bacterial luciferase heterodimer

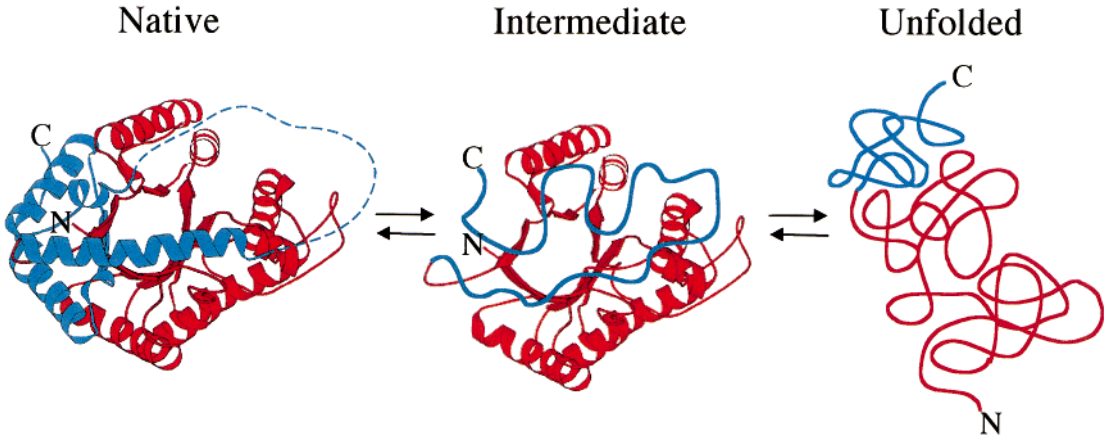

FIGURE 8: Proposed model for unfolding/refolding of the α subunit of bacterial luciferase. The model of the native α subunit is modified from the 1.5 Å heterodimer crystal structure with the disordered loop, residues 262−290, modeled in the dashed blue line (*40*). The proposed N-terminal folding domain, which includes residues 1−235, is shown in red. The proposed C-terminal domain, residues 236−355, is shown in blue. The C-terminal domain in the intermediate becomes unfolded while the N-terminal domain remains folded. In the unfolded state, both domains are unfolded.

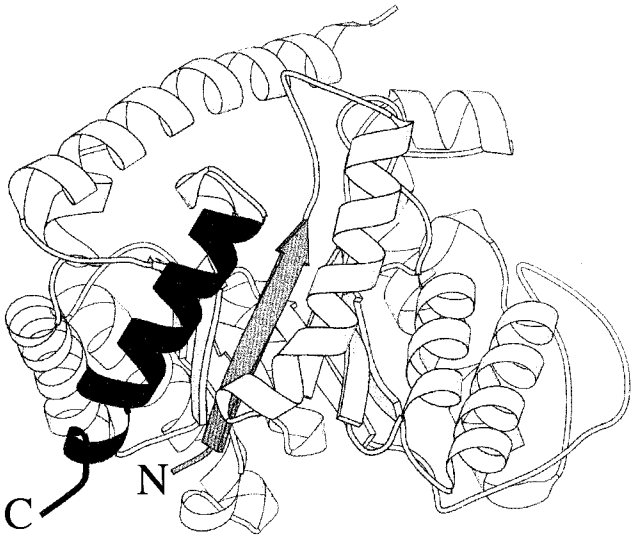

FIGURE 9: α Subunit of bacterial luciferase showing the N and C termini. The N-terminal 34 residues are shown in dark gray and the C-terminal 22 residues are shown in black. The location of the disordered, protease labile loop, indicated in Figure 1A, is at the top of this presentation. This figure was created using the programs SPOCK (*43*, *44*) and MOLESCRIPT (*41*).

(*38*). The three-state unfolding behavior observed in α-TS has been attributed to the sequential unfolding of two domains (*39*). The domain which unfolds at lower concentrations of denaturant is located at the C-terminus of the protein, consisting of α helices 6, 7, 8, and 8′ as well as β strands 7 and 8. The more stable N-terminal domain, comprised of residues 1−188, unfolds at higher concentrations of denaturant. Similar domains have been shown to exist in PRAI (*34*). It appears that the α subunit of bacterial luciferase unfolds in a manner similar to these other TIM-barrel proteins in that some portion of the C-terminus becomes protease labile at the urea concentrations in which the equilibrium folding intermediate is most highly populated. The results reported here, together with the results of folding studies on the other TIM barrel proteins, have allowed us to propose an unfolding model, shown in Figure 8, in which a portion of the C-terminus of the protein unfolds between 0 and 2 M urea followed by the complete unfolding of the remainder of the protein above 4 M urea. Further experimentation will be required to determine whether these portions of the protein may behave as independent domains or subdomains.

It was not surprising to learn that the terminal truncations were occurring from the C-terminal end of the α subunit rather than from the N-terminus. From the examination of the locations of the termini of the α subunit from the heterodimer crystal structure (Figure 9), it can be seen that it would require much less structural rearrangement of the protein to liberate and expose the C-terminus to the action of proteases than the N-terminus. The N-terminus begins in close proximity to the C-terminus at the surface of the protein but then extends deep into the protein's interior to form the first strand of the β barrel from residues 2 to 7. It then emerges as a small surface loop which consists of residues 8−16, which then connects to helix 1. The N-terminal residues from 1 to 34 are shown in dark gray in Figure 9. The C-terminal 22 residues are shown in black in Figure 9. The C-terminal helix consists of residues 333−346 and packs against the outside of the TIM barrel. It is much easier to imagine that the unfolding of the α subunit begins by the unraveling of some part of this C-terminal helix than unfolding from the N-terminus, which would require the partial unfolding of the beta barrel.

On the basis of the results of this study, we propose the model for the unfolding of the α subunit of bacterial luciferase shown in Figure 8. In this model, the protein unfolds to an intermediate state maximally populated at 2 M urea. This intermediate has lost as much as 40% of its secondary structure as well as having a disordered C-terminal region. The intermediate is most likely compact because the tryptophan residues are largely buried and the intermediate has a distinct near-UV circular dichroism spectrum indicative of aromatic groups in a chiral environment. Unfolding from the native to the intermediate state has an associated free energy of 2.24 kcal/mol. Unfolding of the rest of the protein is achieved by 6 M urea. Unfolding of the more stable N-terminal subdomain has an energetic cost of 6.50 kcal/mol.

ACKNOWLEDGMENT

We gratefully acknowledge the Protein Chemistry Laboratory at Texas A&M University. Michael Thomas, Nika van Tilburg, and Jonathan Sparks assisted with the recombinant DNA procedures and Paul Swartz helped with the MOLESCRIPT renditions. We thank the Scholtz lab at Texas A&M University for the use of their circular dichroism spectrometer. We also thank Miriam Ziegler for critical reading of the manuscript.

REFERENCES

1. Anfinsen, C. B. (1973) *Science 181*, 223−230.
2. Wetlaufer, D. B. (1981) *Adv. Protein Chem. 34*, 61−92.
3. Baker, D., and Agard, D. A. (1994) *Biochemistry 33*, 7505−7509.
4. Baldwin, T. O., and Ziegler, M. M. (1992) In *Chemistry and Biochemistry of Flavoenzymes* (Müller, F., Ed.) vol. III, pp 467−530, CRC Critical Reviews in Biochemistry, CRC Press, Boca Raton, FL.
5. Baldwin, T. O., Ziegler, M. M., and Powers, D. A. (1979) *Proc. Natl. Acad. Sci. U.S.A. 76*, 4887−4889.
6. Cohn, D. H., Mileham, A. J., Simon, M. I., Nealson, K. H., Rausch, S. K., Bonam, D., and Baldwin, T. O. (1985) *J. Biol. Chem. 260*, 6139−6146.
7. Johnston, T. C., Thompson, R. B., and Baldwin, T. O. (1986) *J. Biol. Chem. 261*, 4805−4811.
8. Cline, T. W., and Hastings, J. W. (1972) *Biochemistry 11*, 3359−3370.
9. Sinclair, J. F., Waddle, J. J., Waddill, E. F., and Baldwin, T. O. (1993) *Biochemistry 32*, 5036−5044.
10. Fisher, A. J., Raushel, F. M., Baldwin, T. O., and Rayment, I. (1995) *Biochemistry 34*, 6581−6586.
11. Sinclair, J. F., Ziegler, M. M., and Baldwin, T. O. (1994) *Nat. Struct. Biol. 1*, 320−326.
12. Thoden, J. B., Holden, H. M., Fisher, A. J., Sinclair, J. F., Wesenberg, G., Baldwin, T. O., and Rayment, I. (1997) *Protein Sci. 6*, 13−23.
13. Clark, A. C., Sinclair, J. F., and Baldwin, T. O. (1993) *J. Biol. Chem. 268*, 10773−10779.
14. Pace, C. N., Shirley, B. A., and Thompson, J. A. (1989) *Protein Structure, A Practical Approach* (Creighton, T. E. ed.), 311−330, IRL Press, New York.
15. Devine, J. H., Shadel, G. S., and Baldwin, T. O. (1989 *Proc. Natl. Acad. Sci. U.S.A. 86*, 5688−5692.
16. Thomas, M. D., and van Tilburg, A. B. (1999) *Methods Enzymol.* (in press).
17. Laemmli, U. K. (1970) *Nature 227*, 680−685.

18. LeGendre, N., and Matsudaira, P. (1988) *BioTechniques 6*, 154−159.
19. Matsudaira, P. (1987) *J. Biol. Chem. 262*, 10035−10038.
20. Cohn, E. J., and Edsall, J. T. (1943) *Proteins, amino acids and peptides as ions and dipolar ions*, pp 370−381, Reinhold, New York.
21. Laue, T. P., Bhairavi, D. S., Ridgeway, T. M., and Pelletier, S. L. (1992) in *Analytical Ultracentrifugation in Biochemistry and Polymer Science* (Harding, S. E., Rowe, A. J. H., and Horton, J. C., Eds.) pp 63−89, The Royal Society of Chemistry, Cambridge, U.K.
22. Royer, C. A., Mann, C. J., and Matthews, C. R. (1993) *Protein Sci. 2*, 1844−1852.
23. Rausch, S. K., Dougherty, J. J., Jr., and Baldwin, T. O. (1982) in *Flavins and Flavoproteins* (Massey, V., and Williams, C. H., Eds.) pp 375−378, Elsevier North-Holland, Inc., New York.
24. Rausch, S. K. (1983) Ph.D. Thesis, University of Illinois, Urbana, IL.
25. Tanner, J. J., Miller, M. D., Wilson, K. S., Tu, S.-C., and Krause, K. L. (1997) *Biochemistry 36*, 665−672.
26. Baldwin, T. O., Ziegler, M. M., Chaffotte, A. F., and Goldberg, M. E. (1993*) J. Biol. Chem. 268*, 10766−10772.
27. Sinclair, J. F. (1995) Ph.D. Thesis, Texas A&M University, College Station, TX.
28. Baldwin, T. O. (1978) *Methods Enzymol. 57*, 198−201.
29. Baldwin, T. O., Hastings, J. W., and Riley, P. L. (1978) *J. Biol. Chem. 253*, 5551−5554.
30. Holzman, T. F., and Baldwin, T. O. (1980) *Proc. Natl. Acad. Sci. U.S.A. 77*, 6363−6367.
31. Holzman, T. F., Riley, P. L., and Baldwin, T. O. (1980) *Arch. Biochem. Biophys. 205*, 554−563.
32. Clark, A. C. (1994) Ph.D. Thesis, Texas A&M University, College Station, TX.
33. Jasanoff, A., Davis, B., and Fersht, A. R. (1994) *Biochemistry 33*, 6350−6355.
34. Eder, J., and Kirschner, K. (1992) *Biochemistry 31*, 3617−3625.
35. Matthews, C. R., and Crisanti, M. M. (1981) *Biochemistry 20*, 784−792.
36. Crisanti, M. M., and Matthews, C. R. (1981) *Biochemistry 20*, 2700−2706.
37. Sanchez del Pino, M. M., and Fersht, A. R. (1997) *Biochemistry 36*, 5560−5565.
38. Grimsley, J. K., Scholtz, J. M., Pace, C. N., and Wild, J. R. (1997) *Biochemistry 36*, 14366−14374.
39. Miles, E. W., Yutani, K., and Ogasahara, K. (1982) *Biochemistry 21*, 2586−2592.
40. Fisher, A. J., Thompson, T. B., Thoden, J. B., Baldwin, T. O., and Rayment, I. (1996) *J. Biol. Chem. 271*, 21956−21968.
41. Kraulis, P. J. (1991) *J. Appl. Crystallogr. 24*, 946−950.
42. Baldwin, T. O., Christopher, J. A., Raushel, F. M., Sinclair, J. F., Ziegler, M. M., Fisher, A. I., and Rayment, I. (1995) *Curr. Opin. Struct. Biol. 5*, 798−809.
43. Christopher, J. A. (1998) Ph.D. Thesis, Texas A&M University, College Station, TX.
44. Christopher, J. A. (1998) SPOCK: The Structural Properties Observation and Calculation Kit (Program Manual), The Center for Macromolecular Design, Texas A&M University, College Station, TX.
45. Waddle, J. J., and Baldwin, T. O. (1991) *Biochem. Biophys. Res. Commun. 178*, 1188−1193.
46. Choi, H., Tang, C.-K., and Tu, S.-C. (1995) *J. Biol. Chem. 270*, 16813−16819.

BI991449B